Expanded View Figures

Figure EV1. Gating strategies for the assessment of B- and T-cell populations in WT and *Shld2*$^{-/-}$ mice.

A Gating strategies used to quantitate Hardy fractions A-F of progenitor B-cells in bone marrows of WT and *Shld2*$^{-/-}$ mice.
B Gating strategies used to quantitate immature, mature, T1, T2, MZ, and FO B-cell populations in the spleen of WT and *Shld2*$^{-/-}$ mice.
C Gating strategies used to quantitate B1, B2, B1a, and B1b populations in the peritoneal cavity of WT and *Shld2*$^{-/-}$ mice.
D Gating strategies used to quantitate various thymocyte populations in WT and *Shld2*$^{-/-}$ mice.
E Insertion–deletion (indel) penetrance was measured by TIDE sequencing for the lentiCRISPRv2 constructs expressing the indicated sgRNAs targeting the *53bp1*, *Shld1*, *Shld2*, *Shld3*, and *Lig4* genes.
F Baseline GFP frequency of bulk gene-edited A70.2 cells prior to imatinib stimulation (Fig 1F).

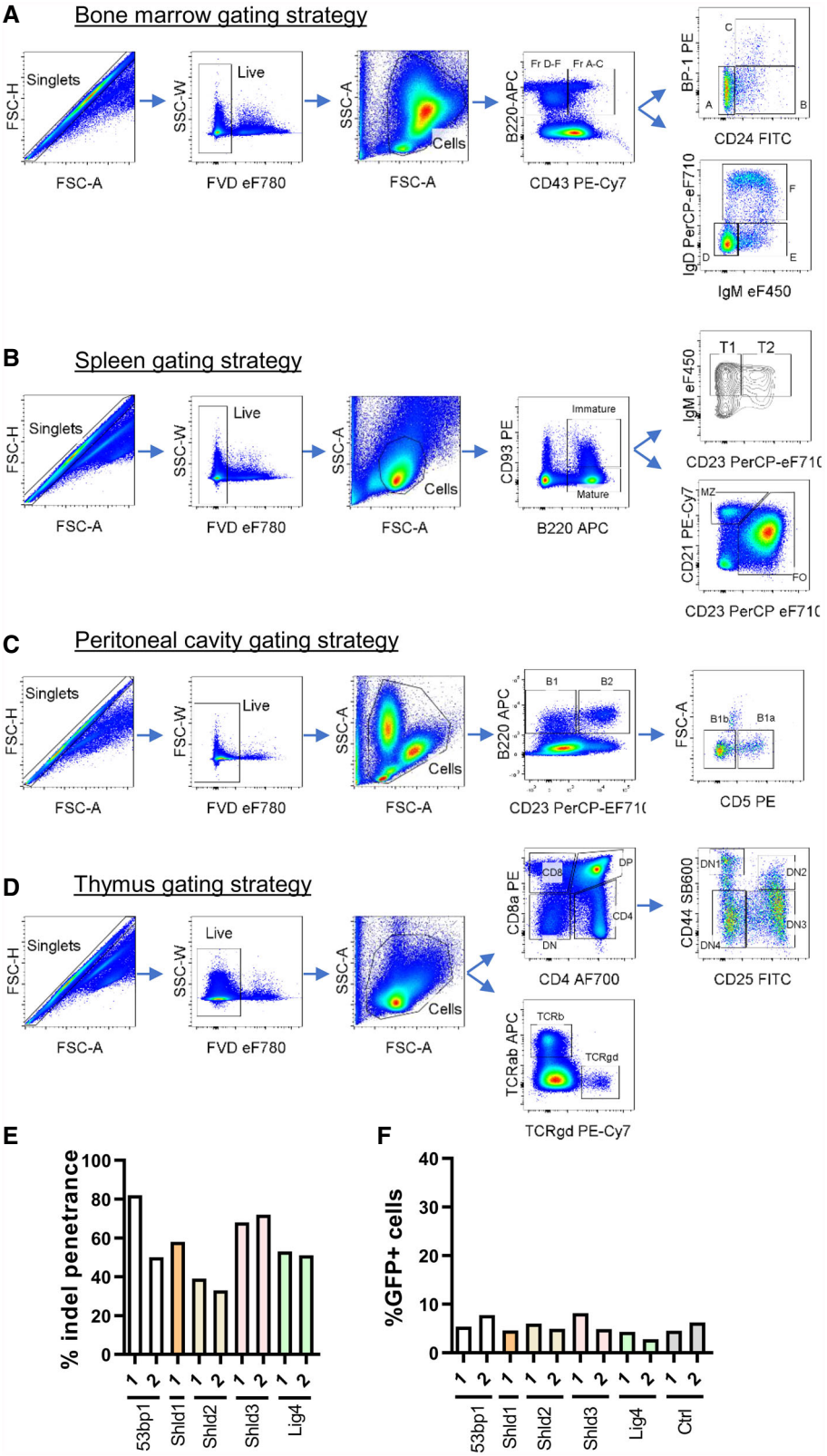
A
Bone marrow gating strategy
Singlets
FSC-H
FSC-A
Live
SSC-W
FVD eF780
Cells
SSC-A
FSC-A
Fr D-F
Fr A-C
B220-APC
CD43 PE-Cy7
BP-1 PE
CD24 FITC
IgD PerCP-eF710
IgM eF450
B
Spleen gating strategy
Immature
Mature
CD93 PE
B220 APC
T1
T2
IgM eF450
CD23 PerCP-eF710
MZ
FO
CD21 PE-Cy7
C
Peritoneal cavity gating strategy
B1
B2
B220 APC
CD23 PerCP-EF710
B1b
B1a
CD5 PE
D
Thymus gating strategy
CD8
DP
CD4
DN
CD8a PE
CD4 AF700
DN1
DN2
DN3
DN4
CD44 SB600
CD25 FITC
TCRb
TCRgd
TCRab APC
TCRgd PE-Cy7
E
% indel penetrance
53bp1
Shld1
Shld2
Shld3
Lig4
F
%GFP+ cells
Ctrl

Figure EV1.

Figure EV2. Sterile transcript or AID protein levels were unaffected in *Shld2*$^{-/-}$ B-cells.

A Representative flow plots of switched *ex vivo* B-cells in Fig 2B.

B Purified splenic B-cells from WT and *Shld2*$^{-/-}$ mice were unstimulated or stimulated for 2 days with LPS + IL4, and germline (sterile) transcripts for Iμ (left panel) and Iγ1 (right panel) were quantitated by qPCR and compared to HPRT mRNA levels. Data are shown relative to WT, which is set at 1.

C Lysates of purified splenic B-cells from WT and *Shld2*$^{-/-}$ mice that were stimulated for 3 days with LPS + IL4 and subjected to Western blot analyses for AID and the internal control β-actin.

D Cas9-induced switching was carried out on *Aid*$^{-/-}$, *Aid*$^{-/-}$ *Lig4*$^{-/-}$, *Aid*$^{-/-}$ *53bp1*$^{-/-}$, and *Aid*$^{-/-}$ *Shld2*$^{-/-/-}$ CH12 clones and switching to IgA was measured 3 days post-transfection. The percent of Ig^{lo} cells is also reported. Transfection with the empty vector pX330 served as negative control. Values are mean frequency ± SD of 3 biological replicates; *$P \leq 0.05$, **$P \leq 0.01$, ***$P \leq 0.001$, ****$P \leq 0.0001$, two-way ANOVA with *post hoc* Dunnett's test.

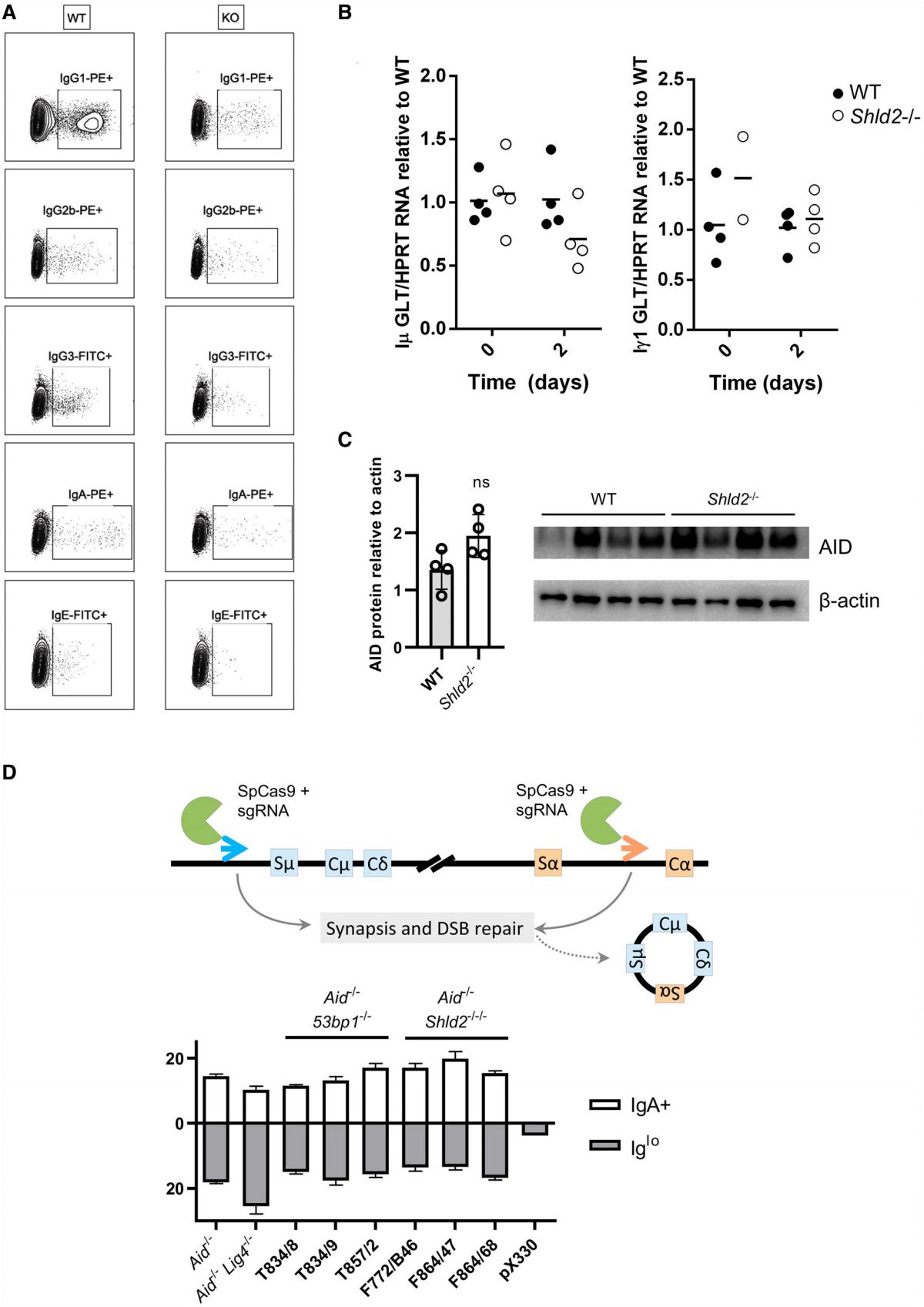
A
WT
KO
IgG1-PE+
IgG2b-PE+
IgG3-FITC+
IgA-PE+
IgE-FITC+
B
Iμ GLT/HPRT RNA relative to WT
Iγ1 GLT/HPRT RNA relative to WT
Time (days)
WT
Shld2-/-
C
AID protein relative to actin
ns
WT
Shld2-/-
AID
β-actin
D
SpCas9 + sgRNA
Sμ
Cμ
Cδ
Sα
Cα
Synapsis and DSB repair
Aid-/- 53bp1-/-
Aid-/- Shld2-/-/-
IgA+
Ig lo
Aid-/-
Aid-/- Lig4-/-
T834/8
T834/9
T857/2
F772/B46
F864/47
F864/68
pX330

Figure EV2.

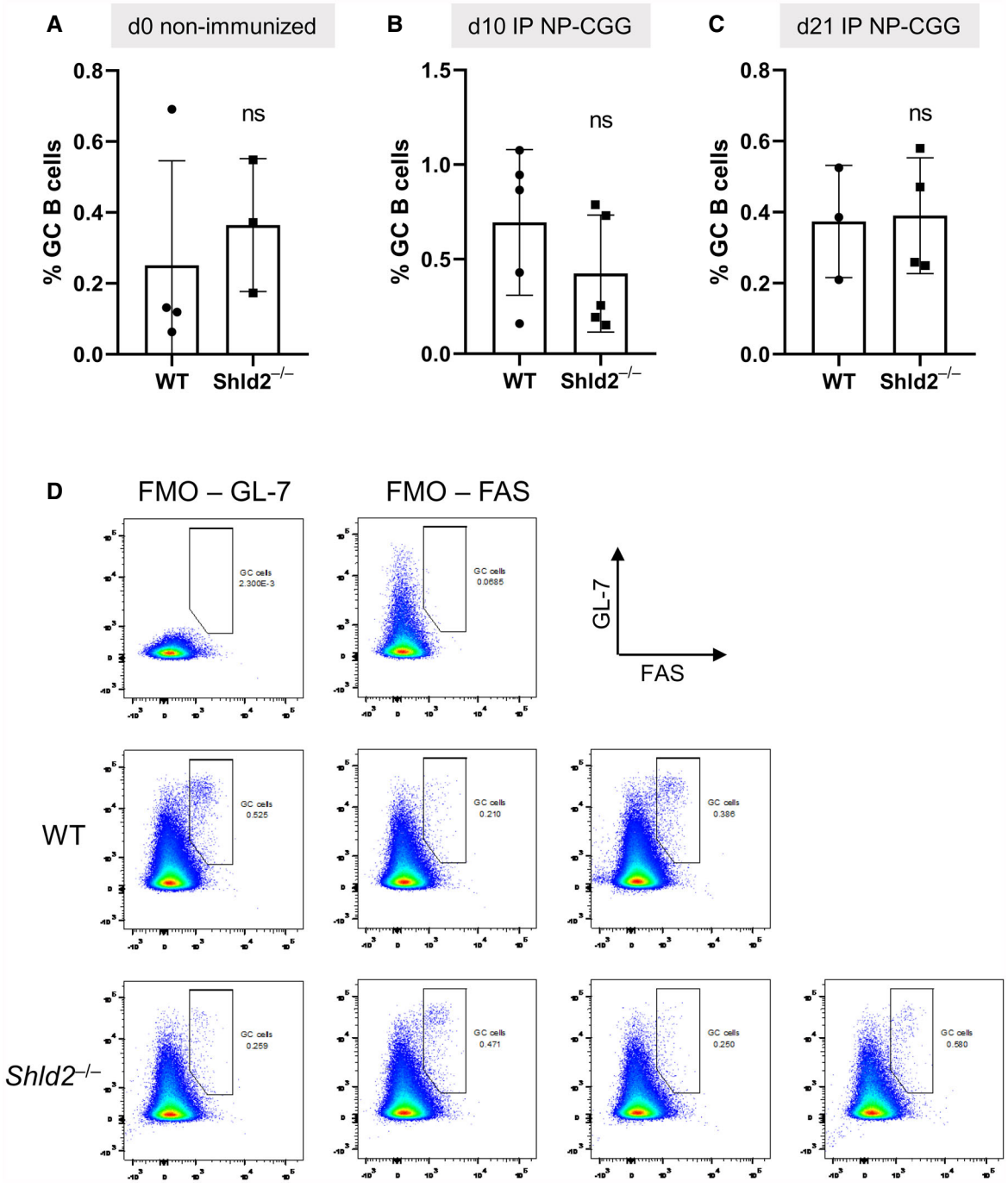

Figure EV3. Germinal center B-cell frequency is not affected by SHLD2 deficiency.

A Germinal B-cell (GL-7$^+$ Fas$^+$) frequency relative to all B-cells (B220$^+$) in the spleen in unimmunized mice; mean ± SD of 3 or 4 biological replicates, ns $P \geq 0.05$, unpaired two-tailed *t*-test.

B As in A, but at day 10 post-NP-CGG immunization; mean ± SD of 4 or 5 biological replicates, ns $P \geq 0.05$, unpaired two-tailed *t*-test.

C As in A, but at day 21 post-NP-CGG immunization; mean ± SD of 3 or 4 biological replicates, ns $P \geq 0.05$, unpaired two-tailed *t*-test.

D Representative flow plots of fluorescence minus one (FMO) controls and day 21 data points.

Figure EV4. CSR induces a permanent loss of Ig expression in CH12 cells.

A The indicated NHEJ-mutant CH12 clones were stimulated with CIT and analyzed by flow cytometry for IgM and IgA expression at days 3 and 7; mean ± SD of 3 biological replicates.

B WT, *53bp1*$^{-/-}$, *Shld2*$^{-/-/-}$, and *Shld3*$^{-/-}$ CH12 clones were stimulated with CIT for 3 days. The IgM^{+}, IgA^{+}, and Ig^{lo} populations were sorted and reanalyzed for expression of IgM and IgA 12 days post-sort. Shown on bar graphs are sorted IgM^{+}, IgA^{+}, and Ig^{lo} populations (each column, 1 technical replicate) from WT and mutant CH12 clones, and the percent of cells expressing IgM, IgA, or low for both isotypes (Ig^{lo}) after 12 days of culture post-sort.

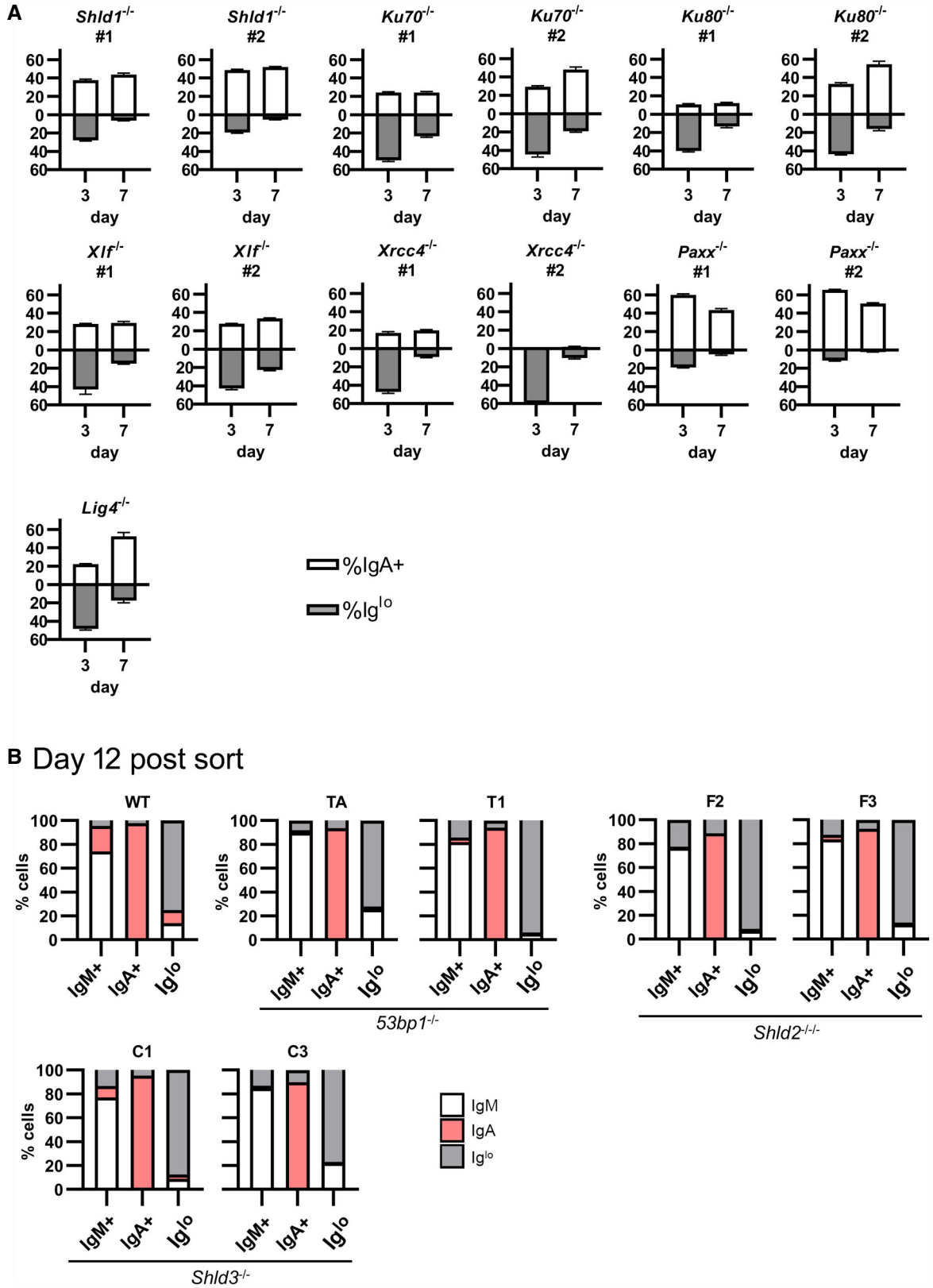

Figure EV4.

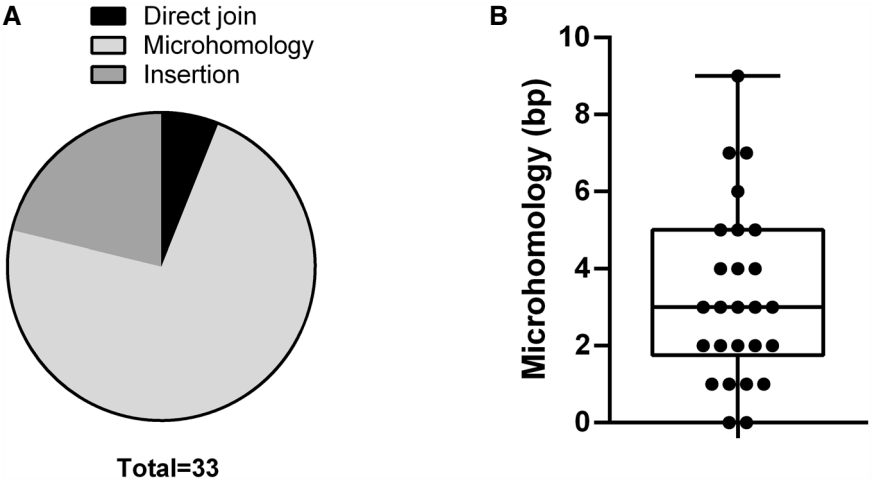

Figure EV5. Repair junctions in Ig^{lo} cells have characteristics of alternative end joining.

A Categorization of *Ighm-Igha* junctions from sequences in Fig 6D, separated into junctions incorporating DNA insertion, microhomology, or neither in the form of direct joins.

B Microhomology distribution of *Ighm-Igha* junctions from sequences in Fig 6D, except for those with insertions (26 independent sequences from one experiment). Median and lower/upper quartiles defined by box, and whiskers represent minimum and maximum values.